Dynamic Response of an Elastic Cylindrical Shell-Solid Core Composite Subject to Time-Dependent Loading

JOHN J. RUMINER*
Lawrence Radiation Laboratory, University of California, Livermore, Calif.

AND

IVOR K. MCIVOR†
The University of Michigan, Ann Arbor, Mich.

A long cylindrical shell bonded to a solid elastic core is subject to external time-dependent loading. The loading is uniform along the generator of the cylinder but may have arbitrary variation around the circumference. The solution is obtained by means of the Laplace transform. Inversion is accomplished by the Residue Theorem, giving the solution in the form of a modal series. Numerical results for impulsive loads demonstrate the wave nature of the motion in the core. The dynamic stress concentration due to the focusing effect is evident. The effect of wave propagation in the core on the motion of the shell varies widely depending upon the material properties of the core. These properties also affect the rate of convergence of the modal solution.

Introduction

THIS paper considers the plane strain dynamic response of an elastic cylindrical shell bonded to a solid core of a different material subject to time-dependent external loading. Of special interest is the wave propagation in the core and its effect on the motion of the shell.

The first investigations pertinent to the present study considered the interaction of a cylindrical shell with an internal liquid.[1,2] The free vibration of a rigid shell bonded to an elastic core has been investigated by Baltrukonis and Gottenberg[3] and Chu.[4] Armenakas[5] formulated the characteristic determinant for the free vibration of a composite elastic cylinder.

More recently Alzheimer, Forrestal, and Murfin[6] obtained the transient response of a hollow core reinforced shell to an axisymmetric impulsive pressure. The solution was obtained by means of the Laplace transform. Inversion was accomplished by employing an asymptotic representation for the transformed solution. This method presents difficulties in the present case of a solid core since the asymptotic representation loses its validity as the wave front passes through the center.

The governing equations for determining the dynamic response to an arbitrary spatial and time-varying external loading are formulated with the equations of linear elasticity for the core and classical thin-shell theory for the cylindrical shell. After a Fourier expansion to remove the circumferential dependence, the solution for each harmonic is obtained by means of the Laplace transform. Inversion is accomplished by means of the Residue Theorem, the poles being along the imaginary axis spaced at the natural frequencies of the composite system. The resulting modal series solution is valid for all time.

Numerical results for impulsive loads demonstrate the feasibility of using the modal solution for examining wave propagation in the core. Dynamic stress concentration due to the focusing effect at the center is evident. The effect of wave propagation in the core on the motion of the shell varies from being a dominant effect to negligible, depending upon the material properties of the core. The material properties can also strongly affect the rate of convergence of the modal solution.

Received January 21, 1971; revision received May 3, 1971. Work performed under the auspices of the U.S. Atomic Energy Commission, suupported by National Science Foundation Grant l-10725.

Index categories: Structural Dynamic Analysis, Structural Composite Materials (Including Coatings).

* Staff Member, Mechanical Engineering Department.

† Professor of Engineering Mechanics.

Formulation

We consider the plane motion of a solid circular cylinder of radius a encased by a thin concentric cylinder of thickness h as shown in Fig. 1. The cylindrical core and casing are composed of different elastic materials. The position of a point in the undeformed core is described by the coordinates $(\bar{r},\theta)$. The radial and tangential components of the displacement are denoted by $\bar{u}$ and $\bar{v}$, respectively. The outer casing is sufficiently thin to be considered as a cylindrical shell of radius a. The position of a point on the undeformed midsurface of the shell is described by the coordinates (a,θ). The radial displacement of a point on the midsurface is denoted by $\bar{w}$, positive inwards, and the tangential displacement is denoted by $\bar{z}$, positive in the direction of increasing θ.

It is convenient to introduce the dimensionless quantities

$$u = \bar{u}/a, \quad v = \bar{v}/a \tag{1a}$$

$$w = \bar{w}/a, \quad z = \bar{z}/a \tag{1b}$$

$$r = \bar{r}/a, \quad \tau = ct/a \tag{1c}$$

where t denotes time, and c is the plate velocity in the shell material. In terms of the shell parameters it is

$$c^2 = E[\rho_s(1 - \nu_s^2)]^{-1} \tag{2}$$

in which E is Young's modulus for the shell material, ρ_s is the shell density, and ν_s is Poisson's ratio.

For the plane motion considered here, the displacement components in the core can be expressed as

$$u = \partial\phi/\partial r + (1/r)\partial\psi/\partial\theta \tag{3a}$$

$$v = (1/r)\partial\phi/\partial\theta - \partial\psi/\partial r \tag{3b}$$

where ϕ and ψ are scalar potential functions. The equations of motion for the core are satisfied if ϕ and ψ satisfy the wave

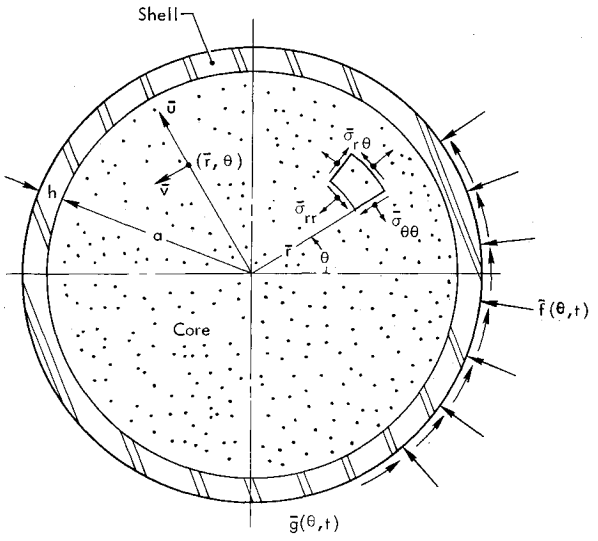

Fig. 1 Core-shell composite showing positive conventions.

equations

$$\partial^2\phi/\partial\tau^2 = \alpha^2\nabla^2\phi \tag{4a}$$

$$\partial^2\psi/\partial\tau^2 = \beta^2\nabla^2\psi \tag{4b}$$

where ∇^2 represents the Laplacian operator in polar coordinates. The quantities α and β are the dimensionless dilatational and shear wave speeds in the core. They are

$$\alpha^2 = (\lambda + 2\mu)/c^2\rho_c \tag{5a}$$

$$\beta^2 = \mu/c^2\rho_c \tag{5b}$$

where λ and μ are the Lamé constants for the core and ρ_c is the core density.

In dimensionless form the equations of motion for the shell[7] are

$$\partial^2 z/\partial\theta^2 - \partial w/\partial\theta + \gamma\partial^3 w/\partial\theta^3 = \partial^2 z/\partial\tau^2 - \eta q_S \tag{6a}$$

$$\partial z/\partial\theta - w - \gamma(\partial^4 w/\partial\theta^4 + \partial^3 z/\partial\theta^3) = \partial^2 w/\partial\tau^2 - \eta q_N \tag{6b}$$

where

$$\gamma = \tfrac{1}{12}(h^2/a^2),\ \eta = a\lambda/c^2 h\rho_s \tag{7}$$

$$q_S = \bar{q}_S/\lambda,\ q_N = \bar{q}_N/\lambda$$

in which $\bar{q}_S$ is the tangential component of the distributed surface loading, positive in the direction of increasing θ, and $\bar{q}_N$ is the normal component, positive when acting inward.

The distributed surface loading on the shell consists of two parts, the surface tractions transmitted across the core-shell interface and the external loading. Thus,

$$q_S = -\sigma_{r\theta}(1,\theta,\tau) + f(\theta,\tau) \tag{8a}$$

$$q_N = \sigma_{rr}(1,\theta,\tau) + g(\theta,\tau) \tag{8b}$$

where f and g are dimensionless external loadings in the tangential and normal directions, respectively. The stress components are normalized with respect to the Lamé constant λ. Finally we must impose displacement continuity at the interface. Thus,

$$w(\theta,\tau) = -u(1,\theta,\tau) \tag{9a}$$

$$z(\theta,\tau) = v(1,\theta,\tau) \tag{9b}$$

The theta dependence may be eliminated by introducing appropriate Fourier representations. A subscript n will denote the nth harmonic of the corresponding variable. Introducing these representations gives the governing equations for the nth harmonic of the core solution as

$$u_n = \phi_n' + n\psi_n/r \tag{10a}$$

$$v_n = -n\phi_n/r - \psi_n' \tag{10b}$$

$$\partial^2\phi_n/\partial\tau^2 = \alpha^2(\phi_n'' + \phi_n'/r - n^2\phi_n/r^2) \tag{10c}$$

$$\partial^2\psi_n/\partial\tau^2 = \beta^2(\psi_n'' + \psi_n'/r - n^2\psi_n/r^2) \tag{10d}$$

$$\sigma_{rr_n} = (\lambda + 2\mu)u_n'/\lambda + nv_n/r + u_n/r \tag{10e}$$

$$\sigma_{\theta\theta_n} = (nv_n/r + u_n/r)(\lambda + 2\mu)/\lambda + u_n' \tag{10f}$$

$$\sigma_{r\theta_n} = (\mu/\lambda)(-nu_n/r + v_n' - v_n/r) \tag{10g}$$

where the prime indicates differentiation with respect to r. Introducing the representations into the shell Eqs. (6) and using the continuity conditions of Eq. (9) yields two additional equations which are effectively boundary conditions for the core solution. They are

$$-n^2 v_n(1,\tau) - nu_n(1,\tau) - \gamma n^3 u_n(1,\tau) = \partial^2 v_n(1,\tau)/\partial\tau^2 - \eta[-\sigma_{r\theta_n}(1,\tau) + f_n(\tau)] \tag{11a}$$

$$nv_n(1,\tau) + u_n(1,\tau) + \gamma[n^4 u_n(1,\tau) + n^3 v_n(1,\tau)] = -\partial^2 u_n(1,\tau)/\partial\tau^2 - \eta[\sigma_{rr_n}(1,\tau) + g_n(\tau)] \tag{11b}$$

The formulation is completed by specifying quiescent initial conditions and requiring the solution to be nonsingular at the origin.

Dynamic Response to Time-Dependent Loading

When the shell-core composite is subjected to external loading, the quantities f_n and g_n in Eq. (11) are known functions of time. Thus, we must solve the field Eqs. (10) subject to the time-dependent boundary conditions, Eq. (11). We effect the solution here by means of the Laplace transform.

Taking the Laplace transform of Eqs. (10c) and (10d) together with quiescent initial conditions gives

$$\hat{\phi}_n'' + \hat{\phi}_n'/r - (n^2/r^2 + s^2/\alpha^2)\hat{\phi}_n = 0 \tag{12a}$$

$$\hat{\psi}_n'' + \hat{\psi}_n'/r - (n^2/r^2 + s^2/\beta^2)\hat{\psi}_n = 0 \tag{12b}$$

where s is the transform variable and the circumflex denotes the transformed function. The solutions of Eq. (12) which are finite at the origin are

$$\hat{\phi}_n = A_n(s)I_n(sr/\alpha) \tag{13a}$$

$$\hat{\psi}_n = B_n(s)I_n(sr/\beta) \tag{13b}$$

where I_n is the modified Bessel function of the first kind and A_n and B_n are functions of s to be determined.

The transformed stress and displacement components are now obtained by transforming (Eqs. 10a,b,e,f) and introducing Eq. (13). We obtain two equations for A_n and B_n by transforming Eq. (11) and introducing the transformed displacements and stresses. The final solution for the transformed displacements has the form

$$\hat{u}_n = [U_n(r,s)\hat{g}_n + \bar{U}_n(r,s)\hat{f}_n]/\Delta_n(s) \tag{14a}$$

$$\hat{v}_n = [V_n(r,s)\hat{g}_n + \bar{V}_n(r,s)\hat{f}_n]/\Delta_n(s) \tag{14b}$$

where $\hat{g}_n$ and $\hat{f}_n$ are the transformed external loadings. The remaining quantities in Eq. (14) are rather lengthy functions of r and/or s involving the modified Bessel functions, the mode number, and the properties of the core and shell. They may be found in detail in Ref. 8.

In the present paper we explicitly consider loading due to normal pressure, taking the external loading as

$$f(\theta,\tau) = 0,\quad g(\theta,\tau) = T(\tau)G(\theta) \tag{15}$$

Thus,

$$f_n = 0,\quad g_n = T(\tau)b_n \tag{16}$$

where b_n denotes the nth Fourier coefficient of the spatial pressure distribution. We first obtain the impulse response; i.e., we let

$$T(\tau) = \delta(\tau) \tag{17}$$

where $\delta(\tau)$ is the Dirac delta function. With this

$$\hat{f}_n = 0, \quad \hat{g}_n = b_n \tag{18}$$

The Laplace inversion integral is

$$h(\tau) = \frac{1}{2\pi i}\int_{\gamma-i\infty}^{\gamma+i\infty} \hat{h}(s)e^{s\tau}ds \tag{19}$$

where γ is a positive constant such that the path of integration lies to the right of all singularities of $\hat{h}(s)$. We close the path of integration by a circular arc extending into the left half of the complex plane. It is shown in Ref. 8 that the integrand vanishes on the circular arc as the radius R tends to infinity. Moreover, the only singularities of the integrand are the zeros of $\Delta_n(s)$, which are simple poles. Thus the Residue Theorem may be employed to evaluate the inversion integral.

On physical grounds we assume that the zeros of $\Delta_n(s)$ lie on the imaginary axis. Thus we set s equal to $i\omega$ and search for the real roots of

$$\Delta_n(i\omega) = 0 \tag{20}$$

Equation (20) is simply the characteristic equation for free vibrations. Moreover it can be shown that if ω_{mn} is a root of Eq. (20), then so is $(-\omega_{mn})$. Thus the poles occur along the imaginary axis at distances equal to the natural frequencies of the system.

Natural Frequencies

A brief discussion of the frequency spectrum of the composite system may be helpful for interpreting the response to time-dependent loadings. The governing equations for free vibration are obtained from Eqs. (10) and (11) by setting f_n and g_n to zero. For each harmonic n, the roots of the characteristic equation were found for two sets of material properties. They were a steel shell bonded to either a glass or a rubber core. The material properties were: for the shell, $E = 30 \times 10^6$ psi, $\gamma_s = 0.29$, $\rho_s = 0.00905$ slugs/in.^{3}; for the glass core, $\lambda = 4 \times 10^6$ psi, $\mu = 4 \times 10^6$ psi, $\rho_c = 0.00290$ slugs/in.^{3}; and for the rubber core, $\lambda = 1.43 \times 10^5$ psi, $\mu = 100$ psi, $\rho_c = 0.00108$ slugs/in.^{3}. Details and representative spectrums can be found in Ref. 8.

For the composite system, there is an infinite spectrum associated with each circumferential mode. The axisymmetric motion is purely dilatational, but for other modes the motion associated with each frequency generally involves both dilation and distortion.

For the case of the glass core, the composite frequencies are small distortions of the core frequencies. The membrane stiffness of the shell is significant but the shell bending stiffness has little influence on the behavior of the composite. For the rubber core, however, a consequence of the low shear modulus of rubber is that the bending mode of the shell plays a prominent role in determining frequencies. Except for the axisymmetric mode ($n = 0$), the motion associated with the first 40 or so frequencies of a given harmonic is almost purely distortional. This has a marked effect on both the response of the system and the convergence of the solution, as discussed later.

Inversion by Means of the Residue Theorem

We first consider the inversion of $\hat{u}_n$ by introducing Eq. (14a) into Eq. (19). The residue at the pole $s = i\omega_{mn}$ is

$$\text{Residue} = \exp(i\omega_{mn}\tau)b_nU_{mn}/iD_{mn} \tag{21}$$

where

$$U_{mn} = U_n(r,i\omega_{mn}) \tag{22a}$$

$$D_{mn} = 1/i(d\Delta_n/ds)|_{s=i\omega_{mn}} \tag{22b}$$

It follows from the Residue Theorem that

$$u_{nI}(r,\tau) = \sum_m b_n[\exp(i\omega_{mn}\tau)U_{mn}(r,i\omega_{mn})/iD_{mn}(i\omega_{mn}) + \exp(-i\omega_{mn}\tau)U_{mn}(r,-i\omega_{mn})/iD_{mn}(-i\omega_{mn})] \tag{23}$$

where m extends over all the natural frequencies and the subscript I denotes the solution as the impulse response. It can be shown that

$$U_{mn}(r,i\omega_{mn}) = U_{mn}(r, -i\omega_{mn}) \tag{24a}$$

$$D_{mn}(i\omega_{mn}) = -D_{mn}(-i\omega_{mn}) \tag{24b}$$

Thus Eq. (23) may be expressed as

$$u_{nI} = \sum_m 2b_n \sin\omega_{mn}\tau \frac{U_{mn}}{D_{mn}} \tag{25}$$

In a similar manner we obtain

$$v_{nI} = \sum_m 2b_n \sin\omega_{mn}\tau \frac{V_{mn}}{D_{mn}} \tag{26}$$

where

$$V_{mn} = V_n(r,i\omega_{mn}) \tag{27}$$

For brevity, the quantities U_{mn}, V_{mn}, D_{mn} are omitted here. They are given in detail in Ref. 8.

For the circumferential mode ($n = 1$), there is an additional pole at $s = 0$. The corresponding solution is the rigid body translation arising from the momentum imparted to the system by a load function containing a nonzero first harmonic. In the subsequent numerical work this pole has been omitted. Thus our solution is measured with respect to a coordinate system moving with the center of mass.

Once the impulse response has been determined, the solution for time-dependent loading may be obtained by convolution. Our interest here is primarily in impulsive type loadings. Thus we consider time dependence of the form

$$T(\tau) = ae^{-b\tau} \tag{28}$$

By suitable choice of the constants a and b, the loading may be varied from an ideal impulse to a step loading. Using the convolution theorem, the solution is

$$u_n(r,\tau) = \int_0^\tau ae^{-bz}u_{nI}(r,\tau - z)dz \tag{29a}$$

$$v_n(r,\tau) = \int_0^\tau ae^{-bz}v_{nI}(r,\tau - z)dz \tag{29b}$$

Carrying out the integration yields

$$u_n = 2ab_n \sum_m (b\sin\omega_{mn}\tau - \omega_{mn}\cos\omega_{mn}\tau + \omega_{mn}e^{-b\tau})\frac{U_{mn}}{(b^2 + \omega_{mn}^2)D_{mn}} \tag{30a}$$

$$v_n = 2ab_n \sum_m (b\sin\omega_{mn}\tau - \omega_{mn}\cos\omega_{mn}\tau + \omega_{mn}e^{-b\tau})\frac{V_{mn}}{(b^2 + \omega_{mn}^2)D_{mn}} \tag{30b}$$

Numerical Results and Discussion

Numerical results were computed for a half cosine spatial loading distribution. Truncating its Fourier series after n equal to 4 gives convergence to within 2% under the point of maximum load at time zero. Thus only the first four nonzero harmonics were retained in the calculations.

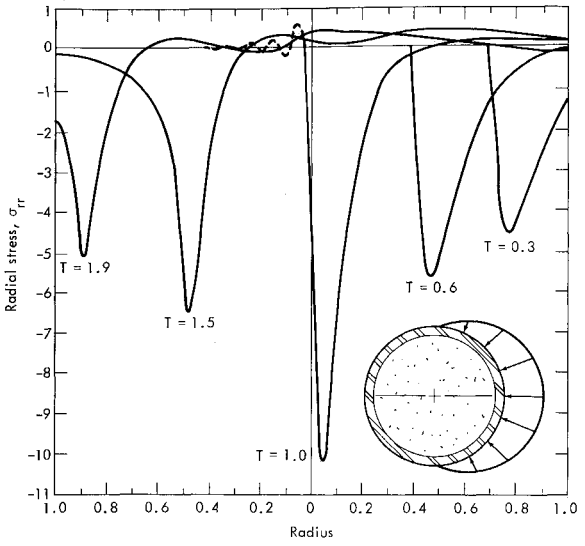

Fig. 2 Radial stress distribution for initial wave in glass core.

The time dependence of the loading is normalized such that

$$\int_0^\infty T(\tau)d\tau = 1 \tag{31}$$

which for Eq. (28) requires that a be equal to b. The decay time was varied, but for the results presented it was chosen so that the amplitude diminished by a factor of 10 in the time that it takes a dilatational wave to travel one tenth the radius of the core.

For each harmonic, 60 roots of the characteristic equation were found by a variation of the half-interval technique. Thus in Eq. (30) we are retaining 60 terms in the summation over m. It was found that for most parts of the solution half that many terms were sufficient for accuracy within a few per cent. The additional terms were required, however, to improve convergence at the wave front. As a check on the numerical calculations, the total energy was computed at each time and compared with the input energy.

Results were computed for a steel shell with a radius-to-thickness ratio of 20 and the two different core materials discussed earlier. The results for the glass core are shown in Figs. 2–6. The time scale has been normalized with respect to the dilatational wave speed in the core; i.e., we

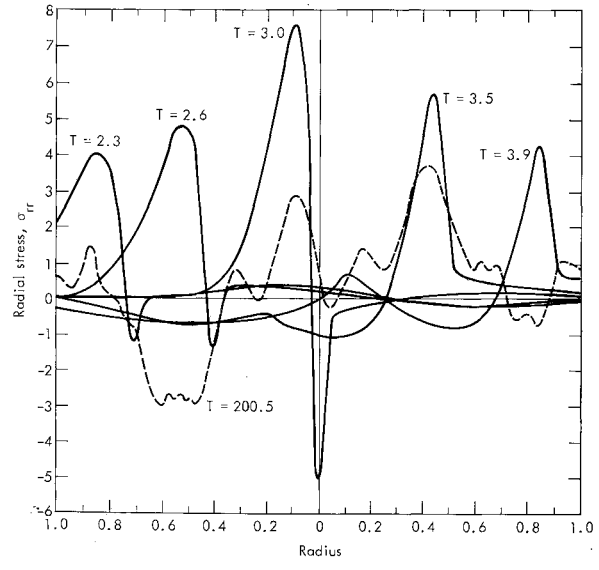

Fig. 3 Radial stress distribution after first reflection and after long time.

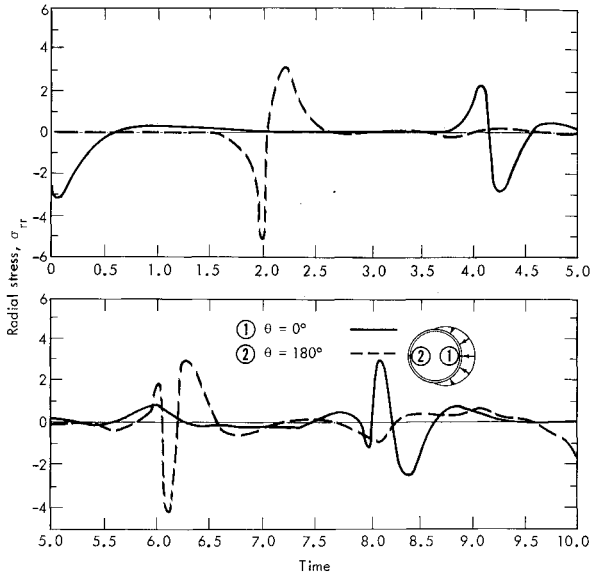

Fig. 4 Normal bond stress for decaying blast load and glass core.

introduce the time

$$T = \alpha\tau \tag{32}$$

This is a convenient scale for picking out wave arrivals, a value of unity being the time for a dilatational wave to travel a distance of one radius.

The wave nature of the modal solution is displayed in Figs. 2 and 3 where the radial stress distribution is shown at different values of T along the diameter emanating from the point of maximum load. Fig. 2 shows the first progression of the wave across the cylinder. The dashed line shows the magnitude of the truncation errors for the stress profile at $T = 1$. These oscillations have been omitted in all other curves presented. The focusing effect causing a high stress concentration at the center is evident. As the wave travels beyond the center the pulse amplitude decreases and appears to be dispersing. This leading portion of the wave is actually due to wave contributions radiating from points other than under the maximum load. The wave emanating from the point of maximum load reflects from the opposite pole at $T = 2$. As the wave front returns across the diameter (Fig. 3), it is characterized by a compressive peak followed by a larger tension wave. The focusing at the center is again evident. Later reflections display a variety of wave shapes with diminishing maximum values of stress. After a large

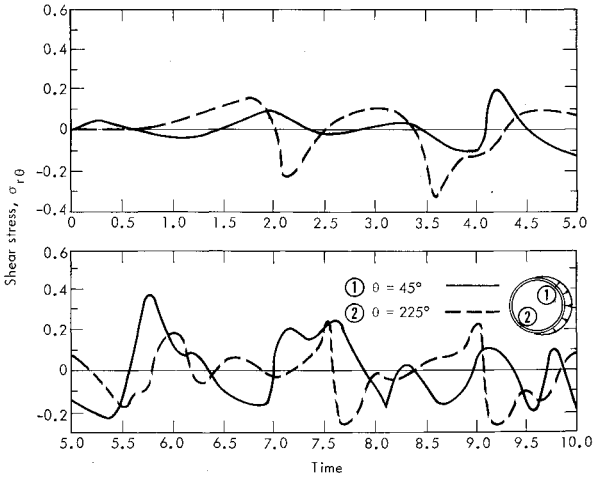

Fig. 5 Bond shear stresses for decaying blast load and glass core.

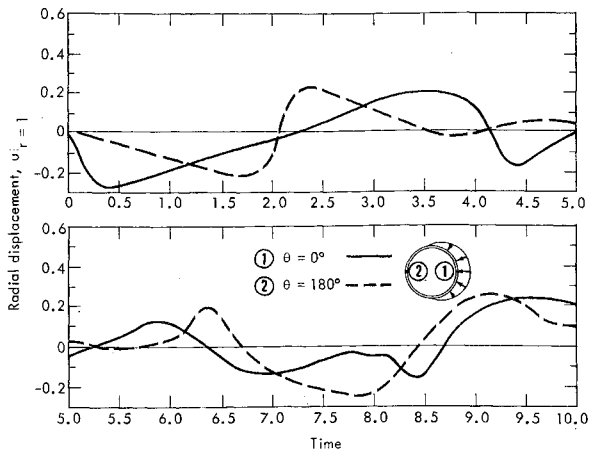

Fig. 6 Radial displacements of shell for decaying blast load.

number of reflections, the wave nature is completely obscured as shown by the dashed line in Fig. 3.

Figure 4 shows the normal bond stress (i.e., the normal stress at the interface) for the point directly beneath the maximum load and the corresponding point at the opposite pole. We note that both the maximum tensile and compressive bond stresses occur at the opposite pole. Similar results for the bond shear stress are shown in Fig. 5. The solid line is for $\theta = 45°$ and the dashed line is for the opposite pole, $\theta = 225°$. For the normal pressure loading considered here, the shear stress is initially small, but after several reflections may increase substantially.

The radial displacement of the shell at the points directly under the maximum load and at the opposite pole are shown in Fig. 6. The effect of the wave propagating through the core can be seen. Omission of the rigid body displacement accounts for the ramp-like behavior of the early response.

Although the analytical form of the solution is the same for the case of a rubber core, the numerical results require a somewhat different interpretation. The form of the solution for a given harmonic of the radial displacement, for example, is

$$u_n(r,\tau) = \sum_m \sin\omega_{mn}\tau R_{mn}(r) \qquad (33)$$

A given radial mode shape R_{mn} is normally associated with both dilatational and distortional motion. For rubber, however, it was found that these effects were highly uncoupled. Because rubber is nearly incompressible, the first dilatational frequency has a high index number m. Further there are from 30 to 40 distortional frequencies between each region of dilatational frequencies. This is shown in Fig. 7 where a dimensionless amplitude of the mode shape for a given radius is plotted vs the integer index m for a typical

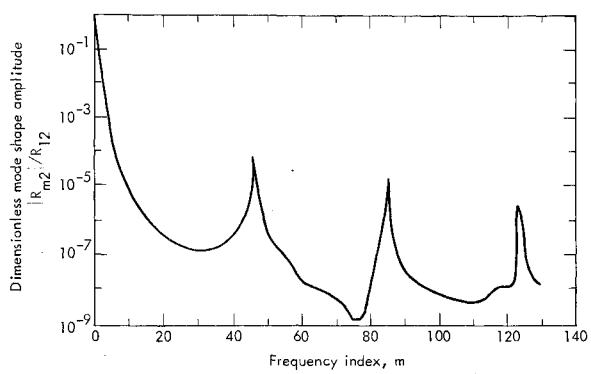

Fig. 7 Dimensionless mode shape amplitude vs frequency index m.

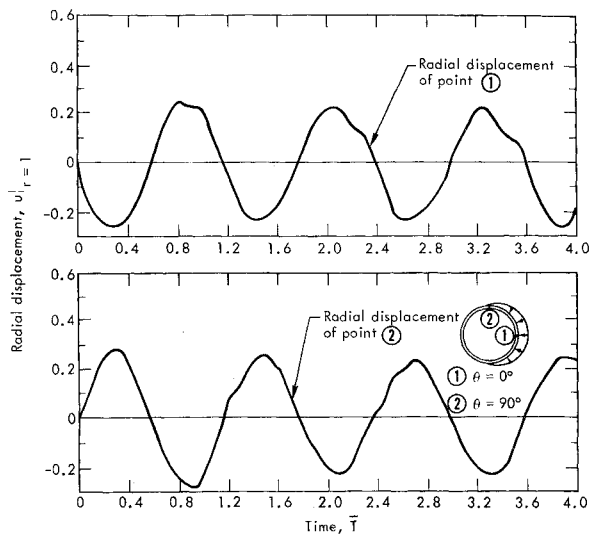

Fig. 8 Radial displacements of shell for decaying blast load and rubber core.

circumferential mode ($n = 2$). The peaks occurring at 45, 85, and 125 are groups of predominantly dilatational modes. The remainder are associated with essentially distortional motion.

Since our series was truncated after 60 terms, only the first group of dilatational modes are included in the solution. This is critical when we seek the initial response of the system. Rubber has a high dilatational wave speed in comparison to the shear wave speed. Their ratio is about 37 to 1 as compared to 1.7 to 1 for glass. Consequently the early time response is due primarily to dilatational waves and their

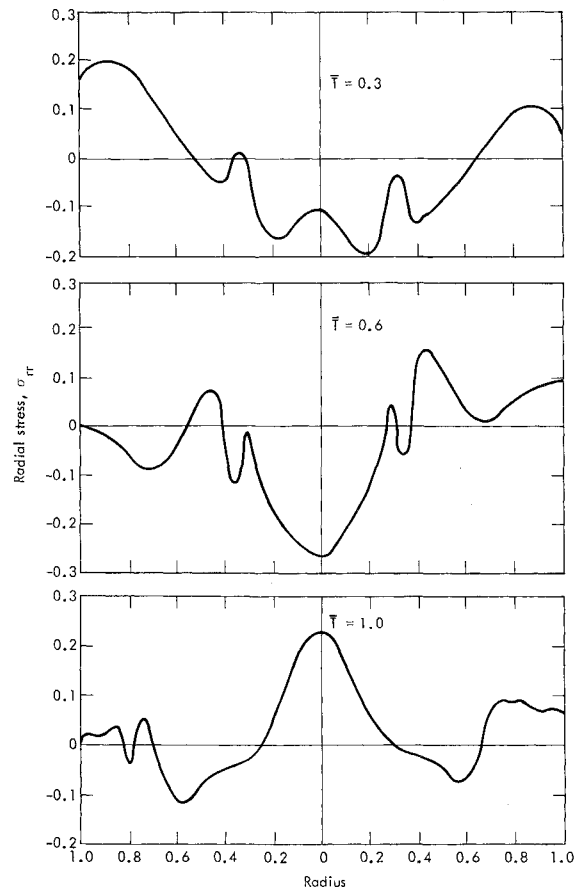

Fig. 9 Radial stress distributions for decaying blast load and rubber core.

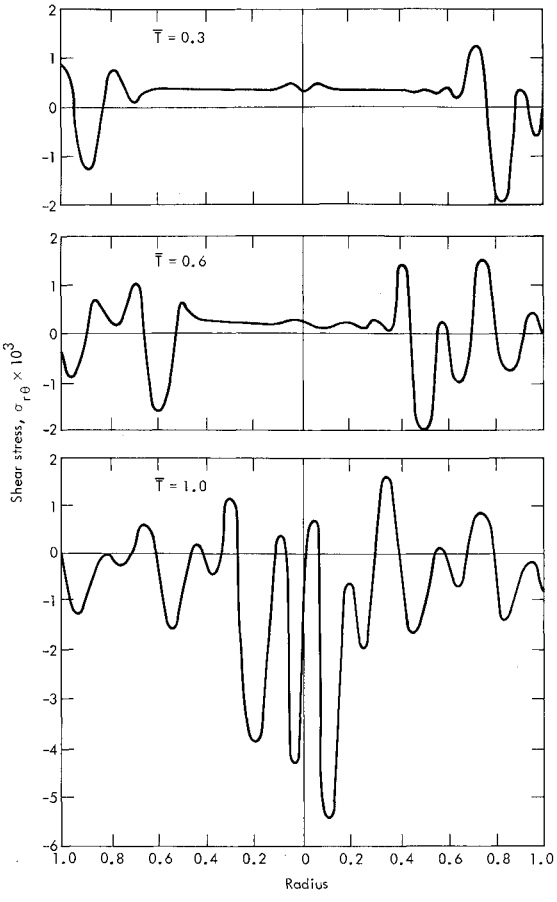

Fig. 10 Shear stress distributions for decaying blast load and rubber core.

reflections. Since the dilatational modes are required to describe this motion, it was found that several hundred terms must be included to obtain acceptable convergence at the wave front.

The present solution (i.e., a solution retaining only 60 terms) does give accurate results except for the very early stage of motion. For small values of time the factor $\sin\omega_{mn}\tau$ in Eq. (33) is small unless ω_{mn} is large. Thus, the high-frequency dilatational peaks contribute the significant terms to the short time solution. As time increases the argument $\omega_{mn}\tau$ becomes large enough for the lower frequencies to become significant. Because the amplitude of the first few distortional modes are several orders of magnitude larger than the rest, they then dominate the solution for all remaining time.

For examining the response after sufficient time has elapsed for the distortional modes to dominate the solution, it is convenient to scale the time with respect to the shear wave speed β. Thus we plot our results for the rubber core with respect to

$$\bar{T} = \beta\tau \tag{34}$$

Figure 8 shows the radial displacement of a shell with radius-to-thickness ratio of 20 as a function of time for the two different points on the midsurface indicated. The displacements are oscillatory, indicating that, in contrast to the previous case, the shell motion is not particularly affected by the wave propagation in the core. Examining the displacements at other points on the circumference verify that the shell is essentially vibrating in the oval ($n = 2$) flexural mode.

The radial stress distribution in the core is shown for the symmetry axis in Fig. 9 for three different times. The results display the long time character found in Fig. 3. Many dilatational reflections have occurred, completely obscuring the wave propagation fronts. A plot of the shear stress, shown in Fig. 10 for the $\theta = 45°$ diameter, does display some wave character in the form of high-frequency oscillations propagating inward with the shear wave velocity. The fact that the wave travels inward from both ends of the diameter indicates that it originates from the reflection of dilatational waves from the boundary rather than the shearing effect of the loading function itself.

References

[1] Berry, J. G. and Reissner, E., "The Effect of an Internal Compressible Fluid Column on the Breathing Vibrations of a Thin Pressurized Cylindrical Shell," *Journal of the Aerospace Sciences*, Vol. 25, 1958, pp. 288–294.

[2] Peralta, L. A. and Raynor, S., "Initial Response of a Fluid-Filled, Elastic, Circular Cylindrical Shell to a Shock Wave in an Acoustic Medium," *Journal of the Acoustical Society of America*, Vol. 36, March 1964, pp. 476–494.

[3] Baltrukonis, J. H. and Gottenberg, W. G., "Transverse Wave Propagation in a Solid Elastic Mass Contained by an Infinitely Long, Rigid, Circular Cylindrical Tank," *Proceedings of the 4th Midwestern Conference on Solid Mechanics*, Univ. of Texas in Austin, Austin, Texas, 1959, pp. 396–414.

[4] Chu, H. N., "Simple Axisymmetric Thickness Vibrations of a Soft Elastic Core Cylinder with a Hard, Thin Elastic Skin," *Journal of the Acoustical Society of America*, Vol. 33, 1961, pp. 1293–1295.

[5] Armenakas, A. E., "Propagation of Harmonic Waves in Composite Circular Cylindrical Shells: Part I, Theoretical Investigations," *AIAA Journal*, Vol. 5, No. 4, April 1967, pp. 740–744.

[6] Alzheimer, W. E., Forrestal, M. J., and Murfin, W. B., "Transient Response of Cylindrical Shell-Core Systems," *AIAA Journal*, Vol. 6, No. 10, Oct. 1968, pp. 1861–1866.

[7] Timoshenko, S. and Woinowsky-Krieger, S., *Theory of Plates and Shells*, McGraw-Hill, New York, 1960, pp. 159–161.

[8] Ruminer, J. J., "The Dynamic Response of a Solid Elastic Cylinder Bonded to a Thin Shell," Ph. D thesis, 1969, Dept. of Engineering Mechanics, The Univ. of Michigan.